

ADAPTIVE MESH REFINEMENT FOR SUPERSONIC MOLECULAR CLOUD TURBULENCE

ALEXEI G. KRITSUK, MICHAEL L. NORMAN, AND PAOLO PADOAN

Department of Physics and Center for Astrophysics and Space Sciences, University of California, San Diego,
 9500 Gilman Drive, La Jolla, CA 92093-0424; akritsuk@ucsd.edu, mnorman@ucsd.edu, ppadoan@ucsd.edu

Revised version September 24, 2018

ABSTRACT

We performed a series of three-dimensional numerical simulations of supersonic homogeneous Euler turbulence with adaptive mesh refinement (AMR) and effective grid resolution up to 1024^3 zones. Our experiments describe nonmagnetized driven supersonic turbulent flows with an isothermal equation of state. Mesh refinement on shocks and shear is implemented to cover dynamically important structures with the highest resolution subgrids and calibrated to match the turbulence statistics obtained from the equivalent uniform grid simulations.

We found that at a level of resolution slightly below 512^3 , when a sufficient integral/dissipation scale separation is first achieved, the fraction of the box volume covered by the AMR subgrids first becomes smaller than unity. At the higher AMR levels subgrids start covering smaller and smaller fraction of the whole volume that scale with the Reynolds number as $Re^{-1/4}$. We demonstrate the consistency of this scaling with a hypothesis that the most dynamically important structures in intermittent supersonic turbulence are strong shocks with a fractal dimension of two. We show that turbulence statistics derived from AMR simulations and simulations performed on uniform grids agree surprisingly well, even though only a fraction of the volume is covered by AMR subgrids. Based on these results, we discuss the signature of dissipative structures in the statistical properties of supersonic turbulence and their role in overall flow dynamics.

Subject headings: ISM: structure — ISM: clouds — hydrodynamics — turbulence — methods: numerical

1. INTRODUCTION

Turbulence in molecular clouds is characterized by very high integral scale Reynolds numbers, $Re \equiv \ell_0 u_0 / \nu \gtrsim 10^8$, where $\ell_0 \approx 10$ pc is the typical scale on which the turbulence is driven, $u_0 \approx 2$ km s⁻¹ is the typical velocity associated with that scale, and ν is the kinematic viscosity of the molecular gas (see Elmegreen & Scalo 2004 for a review). Nonlinear interactions that dominate the dynamics of such multi-scale flows critically depend on adequate resolution and suggest to exploit spatial and temporal adaptivity in numerical simulations. While adaptive mesh refinement has previously been applied to simulate the evolution of individual singular structures in incompressible Euler turbulence (Pumir & Siggia 1990; Grauer, Marliani, & Germaschewski 1998), no attempts have been made so far to address the isotropic turbulence case with AMR.

In this letter we apply high order adaptive methods to simulate supersonic turbulence in star forming molecular clouds with very high resolution. Such simulations are essential for understanding the nature of turbulent fragmentation that may ultimately control the stellar initial mass function (Padoan & Nordlund 2002). We exploit the fact that turbulent flows are not completely chaotic. Order is always present on both large and small scales due to the intermittent nature of turbulence. For instance, large under-dense voids and sharp density peaks are known to be characteristic of supersonic turbulent flows with a “soft” equation of state (Passot & Vázquez-Semadeni 1998). We therefore expect AMR simulations of isothermal turbulence to be beneficial in terms of computational resources.¹ We show that in fact AMR technique can be profitably applied to turbulence simulations in contrast with the prevailing *belief* that in such

studies the adaptive mesh does not help as the fine structures emerge through the entire computational domain.

2. TURBULENCE, INTERMITTENCY, AND ADAPTIVE MESHES

It follows from the Kolmogorov (1941) phenomenology for turbulent cascade (K41) that the inertial range spans an interval of scales $\mathcal{N} \equiv \ell_0 / \eta \sim [\nu^3 / (\ell_0^3 u_0^3)]^{-1/4} \sim Re^{3/4}$, where $\eta \sim (\nu^3 / \varepsilon)^{1/4}$ is the Kolmogorov dissipation scale, and the energy cascade rate $\varepsilon \sim u_0^3 / \ell_0$. Hence, the number of zones per integral scale ℓ_0^3 required to model a three-dimensional turbulent flow using a finite-difference method is $\mathcal{N}^3 \propto Re^{9/4}$. The storage resource for a numerical experiment of this sort would also grow as $\mathcal{S} \propto Re^{9/4}$, while the number of CPU hours needed to simulate high-Reynolds-number flows on a uniform grid for a given number of large eddy turnover times would scale as $\mathcal{T} \propto Re^3$ (e.g. Frisch 1995).

However, the above calculation implicitly assumes that the inertial range flow is completely chaotic and does not contain any coherent structures, which is often not the case in experimental high- Re flows. In fact, both laboratory experiments and numerical simulations indicate the presence of some order in the flows on both small $\ell \sim \eta$ and large $\ell \sim \ell_0$ scales. Since turbulence is intermittent, the K41 theory gives only an approximation to its statistical properties and requires corrections to reproduce experimental measurements of high-order statistics. One way to add a form of intermittency to the K41 model is known as the β -model (Frisch, Sulem, & Nelkin 1978). It assumes that the fraction of the space occupied by the ‘active’ eddies of size ℓ scales as $(\ell / \ell_0)^{3-D}$, where D is interpreted as the fractal dimension of small-scale dissipative structure. In the framework of the β -model the dissipation scale is a function of D , therefore $\mathcal{N}_D \equiv \ell_0 / \eta(D) \sim Re^{3/(1+D)}$. One can easily recover the familiar K41 result from this formula by setting $D = 3$ which corresponds to the zero-intermittency limit. Thus, the scaling

¹ Application of AMR techniques to multiphase interstellar turbulence simulations, where the effective adiabatic index determined by the balance between heating and cooling at high densities falls below unity, appears to be even more promising.

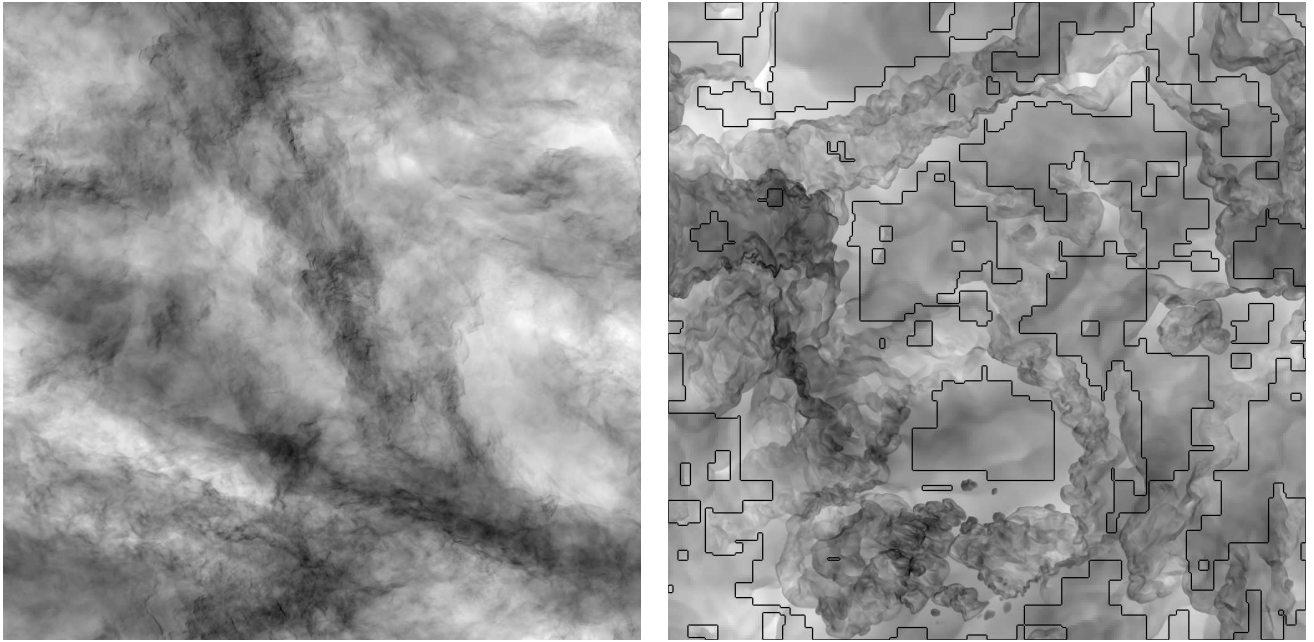


FIG. 1.— Gas density from AMR simulation of supersonic Mach 6 turbulence with effective resolution of 1024^3 at time $t = 6 t_{dyn}$. *Left panel:* a projection of the density field through the computational box (log scale, dense regions are dark). *Right panel:* a thin slice from the same density distribution with contours showing the patches of the base grid *not* covered by the AMR subgrids. The total volume covering factor of the first level AMR subgrids is approximately 65%.

for the storage depends on the fractal dimension of the small-scale dissipative structure, $S_D \propto Re^{3D/(1+D)}$.

There are good reasons to assume $D \approx 1$ in the incompressible case, where vortex filaments are the most singular dissipative structures (She & Lévéque 1994; Dubrulle 1994), and $D \approx 2$ for supersonic compressible turbulence, where the dissipative structures are shocks (Boldyrev 2002). For these fractal dimensions, $S_1/S \sim Re^{-3/4}$ and $S_2/S \sim Re^{-1/4}$, so the advantage of adaptive methods for simulations of high- Re turbulent flows is quite clear.

There is a simple direct analogy between the process of building an AMR hierarchy to resolve the turbulent structures of the fractal dimension D and the box-counting method for determination of that same fractal dimension. The fractal dimension is given by the relation $n(\delta) \propto \delta^{-D}$, where $n(\delta)$ is the number of boxes of linear size δ needed to cover the set of singular structures. One can think of the box size δ as a function of the level number l in the AMR hierarchy, $\delta_l = \delta_0 f^{-l}$, where δ_0 is the zone size on the base grid and f is the refinement factor (usually $f = 2$ or 4). Then the number of zones needed to cover the structures on level l would grow as $n_l \propto \delta_l^{-D} \propto f^{lD}$, and the volume covering factor of level l subgrids would scale with the level number as $F_l \propto f^{l(D-3)}$. Assuming $D = 2$, one gets $F_l \propto f^{-l}$. Having chosen an appropriate resolution for the base grid and $f = 4$, one can predict the covering factors for $l = 1, 2$, and 3 -subgrids to be $0.25, 0.06$, and 0.015 , respectively. For incompressible turbulence, the same factors are valid if $f = 2$.

At what base grid resolution AMR first becomes beneficial for turbulence simulations? As with the box-counting method, the expected scaling can be attained only with a high enough resolution. It is necessary to provide integral/dissipation scale separation for the inertial range to become extended in the wavenumber space. In simulations of compressible Euler turbulence with PPM this can be achieved at resolutions somewhere in between 256^3 and 512^3 (schemes with higher numerical diffusivity than PPM would require many more zones), while for compressible Navier-Stokes tur-

bulence one needs about 4^3 times higher resolution since a larger range of scales is needed to account for the physical dissipation (Sytine et al. 2000). Therefore, in PPM simulations of Euler turbulence the advantage of AMR comes into play earlier than in those of Navier-Stokes turbulence. On the other hand, due to the difference in scaling behavior, AMR is expected to save more resources in numerical experiments with incompressible flows at very high Reynolds numbers. In the following sections we show that in practice for Mach 6 isothermal turbulence the advantage of AMR is indeed first noticeable at a resolution of about 512^3 , and the scaling relations derived above are consistent with our numerical experiments which involve the *Enzo* code (O’Shea et al. 2004, and references therein).

3. NUMERICAL APPROACH

The *Enzo* code uses a direct Eulerian formulation of the Piecewise Parabolic Method (Colella & Woodward 1984, PPM) to solve the equations of gas dynamics on a hierarchy of structured adaptive meshes (Berger & Colella 1989).

In order to mimic the conditions in molecular clouds, we adopt a quasi-isothermal equation of state with the ratio of specific heats $\gamma = 1.001$. To test our PPM implementation in this highly compressible low- γ regime and at high Mach numbers, we ran a number of tests with and without AMR, including simple shock tube tests described in (Balsara 1994). We found very good agreement with the exact solutions and with results obtained with a Riemann solver for purely isothermal gas dynamics. The temperature variations in tests with Mach 6 flows, due to the small deviation of γ from unity, were typically below 0.1%.

The AMR subgrids are placed where needed to resolve shocks with large pressure jumps and regions of strong shear. We identify shocks using the PPM shock detection algorithm. In addition, we also use a norm of the velocity gradient matrix $\|\partial_i u_j\|$ to account for shear. This matrix norm is similar to the Frobenius norm, except that it does not include the contribution from diagonal elements. To get a better AMR

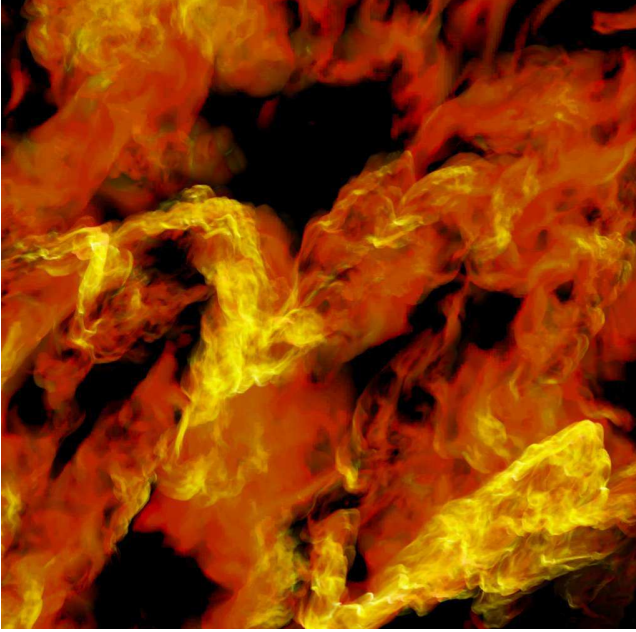


FIG. 2.— Volumetric rendering of the gas density in a 100-zone-thick slice through a subsample of the computational domain. V- and U-shaped shocklets or “Mach cones” are the most common structures in supersonic isothermal hydrodynamic turbulence. As in a hierarchy of vortices in incompressible turbulence, large-scale Mach cones are broken into smaller and smaller ones down to the finest resolved scale. Mach angles of the largest cones visible in this snapshot correspond to relative fluid velocities of $(2-3)c_s$.

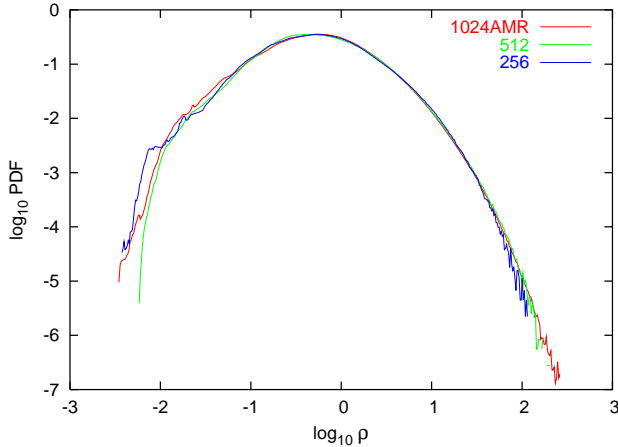


FIG. 3.— Comparison for turbulence statistics based on 256^3 and 512^3 uniform grid simulations and an AMR simulation with effective grid resolution of 1024^3 at time $t = 6 t_{dyn}$. Probability density functions (PDFs) for the gas density.

efficiency for simulations of turbulent flows (which involve a large number of subgrids) we use mesh refinement by a factor of 4. We obtained a very good agreement between our non-adaptive and AMR runs for refinement on shocks with pressure jumps $\Delta p/p \geq 2$. When a combination of shocks and shear controlled the refinement, a minimum pressure jump of 3 was sufficient, while the application of the second refinement criterion accounted for some 20% more zones to be flagged. Note that these values are given only for orientation, while the actual lower bound for pressure jumps in refined shocks would depend on the AMR implementation.

To maintain the turbulent kinetic energy in the computational box at a given level, we use large-scale solenoidal force per unit mass with a fixed spatial pattern and a constant power in the range of wavenumbers $k \in [1, 2]$.

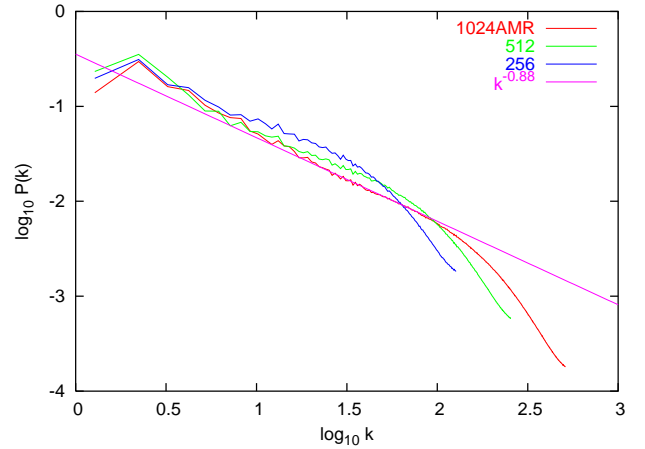


FIG. 4.— Same as in Fig. 3, but for the gas density power spectra.

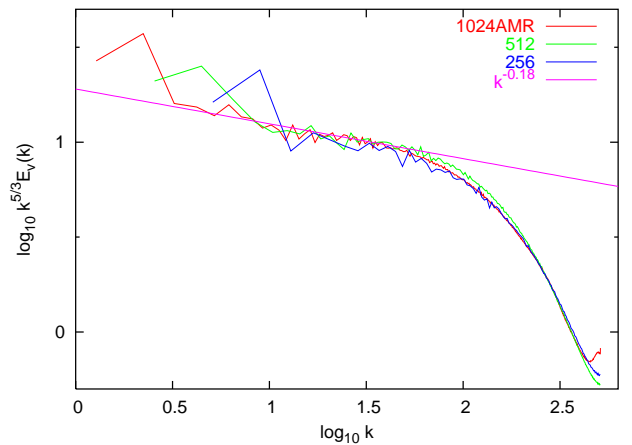


FIG. 5.— Same as in Fig. 3, but for the compensated total velocity power spectra, scaled so that the curves match in the numerical dissipation range of PPM where they are invariant.

4. TURBULENT STRUCTURES AT HIGH RESOLUTION

We first performed a series of nonadaptive simulations of driven turbulence with an rms Mach number of 6 varying the uniform grid resolution from 128^3 up to 512^3 zones. We started the simulations with a uniform gas density and ran them for 6 dynamical times² to follow the development and saturation of the turbulent flow. We then restarted the 128^3 run as an AMR simulation with the base grid of 128^3 and one level of refinement by a factor of 4, ran it from 4.8 to $6 t_{dyn}$, and compared the results with our uniform grid run with the equivalent resolution of 512^3 zones. After a few iterations we found that refinement on shocks with pressure jumps above ≈ 2 gives us velocity power spectra consistent with the spectra from nonadaptive run with the same effective resolution. The velocity statistics appear to be more sensitive to the refinement criterion than the density PDF or the density power spectrum. Since the volume covering factor of the first level subgrids in this AMR simulation was about 90%, it remained unclear whether it is the high covering fraction that provides convergence or it is indeed the right refinement criterion. Before switching to higher resolution base grids (it is wasteful to run AMR covering 90% of the volume) we restarted the same AMR run from $t = 6 t_{dyn}$ allowing for two levels and got an estimate of the covering fraction for the second level about

² $t_{dyn} \equiv L/(2M)$, where L is the box size, M is the rms Mach number, and the sound speed c_s is unity.

34% at effective resolution of 2048^3 . This number should be considered as a lower limit since it will grow by a few percent over the following t_{dyn} , while the flow gets fully resolved on the second level.

We then repeated the same experiment with the 256^3 base grid and one level of refinement, with however a slightly different refinement recipe which also included shear, see Section 3 for details. With effective resolution of 1024^3 this AMR run is the largest simulation to date of supersonic turbulence in molecular clouds. Fig. 1 shows a snapshot of the gas density field from this run. From the left panel, where we show a distribution of the column density, it may indeed look like the fine structures emerge through the entire computational domain. However, the morphology of the projected density field is quite different from what one can see in a slice, highlighting a significant loss of information built into the projection procedure. As one can see from a thin slice through the box shown in the right panel, AMR does help in this case since turbulence is very intermittent. The first level subgrids do not cover the under-dense voids and also some smaller windows in the high and intermediate density gas where the strong shocks are absent. These regions do not contribute much to cascading the energy from large to small scales as their share in the turbulence statistics is the same whether they are refined or not. Strong shock interactions and associated nonlinear instabilities create a very sophisticated multiscale pattern in the dynamically active regions (Figs. 1, 2) that is morphologically similar to what is observed in molecular clouds. This pattern is missing in numerical simulations at lower Re . We identify Mach cones and U-shaped shocklets as self-similar elements of this pattern (Fig. 2). These effects of nonlinear shear instabilities resolved in our simulations can explain the lack of large-scale shock signatures in the observations of molecular gas by Brunt (2003).

While we do not have an equivalent nonadaptive simulation, the comparison with PDFs and power spectra from 256^3 and 512^3 runs shown in Figs. 3 – 5 speaks for itself. The density PDFs can be very precisely fitted by a log-normal distribution and the AMR data match those from the two nonadaptive runs, although the superior resolution of the AMR run provides better sampling for the high end of the density distribution. Interactions of strong counter-propagating shocks are responsible for intermittent oscillations in the high density wing of the PDF, which are well resolved in our AMR simulation. These interactions also cause transient strong rarefactions lagging behind in time. As a result, on time-scales short compared to the dynamical time, the density PDF slightly wanders around its average log-normal representation at the highest densities and displays large temporal oscillations in its low-density end, see Fig. 3. The same processes reveals itself in correlated variations of the three-dimensional power spectrum of density in the inertial range. The slope lies somewhere between -0.8 and -0.9 in our nonmagnetized models, see Fig. 4. The spectrum gets shallower upon the collisions of strong shocks, when the PDF's high density wing rises above

the average log-normal representation.

The density power spectrum builds up quickly at high wavenumbers, after we switch the AMR machinery on, simply because PPM starts resolving the shocks better. However, the relaxation of the velocity power proceeds slower since it takes about one dynamical time for the resolved local sharp density structures to get through nonlocal dynamical interactions involving multiple scales. Only then the inertial range really extends to smaller scales. When AMR is first activated, the velocity power is insufficient at $k \gtrsim 25$ and scales approximately as k^{-2} in this range. It then steadily accumulates at those frequencies for about t_{dyn} and saturates exactly at the level predicted by our nonadaptive simulations, see Fig. 5. The slope of the velocity power spectrum for the snapshot shown is about -1.85 , i.e. somewhat steeper than a slope of -1.74 predicted by Boldyrev (2002) for supersonic turbulence assuming $D = 2$ and assuming the third order structure function exponent equal to unity, as in incompressible turbulence.³ According to the formalism developed by Dubrulle (1994), a slope of -1.85 would imply $D \approx 2.3$. This is consistent with the dimensionality of dissipative structures that can be independently estimated using the volume covering fractions of AMR subgrids at different levels of resolution (90 , 65 , and 34% at 512^3 , 1024^3 , and 2048^3 , respectively). Such estimate returns the same value of $D \approx 2.3$. Within the uncertainties, both independent estimates agree with the observationally determined fractal dimension of molecular clouds $D = 2.3 \pm 0.3$ (Elmegreen & Falgarone 1996).

5. CONCLUSIONS

While details of AMR implementation may vary and may have to be further refined to reproduce higher order statistics, it is clear that adaptivity in both space and time is indispensable for numerical experiments with homogeneous isotropic supersonic turbulence at very high Reynolds numbers with grid resolutions $\gtrsim 1024^3$.

Our simulations reveal a pattern of small-scale structures that is completely missing at lower Re . These structures originate in nonlinear instabilities inherent in isothermal supersonic flows and may control the scaling properties of turbulence and the fractal dimension of the dynamically important structures. Since the presence of magnetic fields can modify the unstable modes, it cannot be taken for granted that magnetized turbulence should have the same scaling properties.

Numerical experiments at very high Reynolds numbers are crucial for studies of turbulence in molecular clouds.

This work was partially supported by NRAC allocation MCA098020S and utilized computing resources provided by the San Diego Supercomputer Center.

³ Averaging over independent realizations of the turbulent flow is needed to obtain reliable estimates for the scaling exponents. This lies outside the scope of this letter which is primarily focused on the applicability of adaptive methods.

REFERENCES

- Balsara, D. S. 1994, ApJ, 420, 197
 Berger M. & Colella, P. 1989, J. Comp. Phys., 82, 64
 Boldyrev, S. 2002, ApJ, 569, 841
 Brunt, C. M. 2003, ApJ, 583, 280
 Colella, P. & Woodward, P. R. 1984, J. Comp. Phys., 54, 174
 Dubrulle, B. 1994, Phys. Rev. Lett., 73, 959
 Elmegreen, B. G. & Scalzo, J. 2004, ARA&A, 42, 211
 Elmegreen, B. G. & Falgarone, E. 1996, ApJ, 471, 816
 Frisch, U. Turbulence, Cambridge University Press, 1995
 Frisch U., Sulem P.L., & Nelkin M. 1978, J. Fluid Mech., 87, 719
 Grauer R., Marliani C., & Gernaschewski K. 1998, Phys. Rev. Lett., 80, 4177
 Kolmogorov, A. N. 1941, Dokl. Akad. Nauk SSSR, 30, 299 (K41)
 O'Shea, B. W., Bryan, G., Bordner, J., Norman, M. L., Abel, T., Harkness, R., & Kritsuk, A. G. 2004, astro-ph/0403044
 Padoan, P. & Nordlund, Å. 2002, ApJ, 576, 870
 Passot, T., & Vázquez-Semadeni, E. 1998, Phys. Rev. E, 58, 4501

- Pumir A. & Siggia E., 1990, Phys. Fluids A, 2, 220
She, Z.-S., & Lévéque, E. 1994, Phys. Rev. Lett., 72, 336
Sytine I.V., Porter D.H., Woodward P.R., Hodson S.W., & Winkler K.-H.,
2000, J. Comp. Phys., 158, 225